Available online at www.sciencedirect.com
SCIENCE DIRECT
ELSEVIER
Geomorphology 75 (2006) 283–299
GEOMORPHOLOGY
www.elsevier.com/locate/geomorph

Assessing the relative efficiency of fluvial and glacial erosion through simulation of fluvial landscapes

Simon H. Brocklehurst [a,*], Kelin X. Whipple [b]

[a] School of Earth, Atmospheric and Environmental Sciences, The University of Manchester, Manchester M13 9PL, UK
[b] Department of Earth, Atmospheric and Planetary Sciences, Massachusetts Institute of Technology, Cambridge MA 02139, USA

Accepted 27 July 2005
Available online 9 November 2005

Abstract

The relative rates of erosion by rivers and glaciers, and the topographic effects of these two different styles of erosion, remain outstanding problems in geomorphology. We use a quantitative description of local fluvial landscapes to estimate how glaciated landscapes might look now had glaciers not developed. This indicates the landscape modification attributable to glacial erosion. We present examples from the Sierra Nevada, California and the Sangre de Cristo Range, Colorado. In smaller drainage basins, glacial modification is focussed above the mean Quaternary equilibrium line altitude (ELA), where both ridgelines and valley floors have been lowered as a consequence of glaciation. At lower elevations, small glaciers have apparently widened valleys without incising the valley floor beyond what a river would have. This may reflect the short residence time of the glaciers at their full extent, or differences in the subglacial drainage network between the glacier margins and the thalweg. In larger drainage basins, the pattern of glacial erosion is dramatically different. Here, the glaciers have modified longitudinal profiles, as well as valley cross sections, far below the mean Quaternary ELA. Possible causes of this difference in the larger basins include the larger accumulation area, greater shading of the valley floor, longer residence times for ice at its full extent, and the influence of the shallower valley slope prior to glaciation on the subsequent glacier and subglacial drainage conditions.

Keywords: Glacial erosion; Landscape evolution

1. Introduction

Glaciers are responsible for carving some of the most spectacular landscapes on Earth, and they play a crucial role in hypotheses relating late Cenozoic climate change, erosion, and geodynamics (Hallet et al., 1996; Molnar and England, 1990; Raymo and Ruddiman, 1992; Raymo et al., 1988; Whipple et al., 1999). Such hypotheses cannot be addressed without considering the effects of the transition from fluvial to glacial erosion as a result of climatic cooling. In this context, it is surprising that little is known about the rates of erosion achieved by glaciers, and even less about the distribution of this erosion in either space or time. Here, we employ a locally calibrated model of the fluvial landscape to suggest how modern landscapes would look had glaciers never developed, and deduce the relative rates and patterns of erosion attributable to glaciers.

Most studies designed to evaluate relative rates of fluvial and glacial erosion have focussed on measuring short-term rates of erosion from sediment yields.

* Corresponding author. Fax: +44 161 275 3947.
E-mail address: shb@manchester.ac.uk (S.H. Brocklehurst).

0169-555X/$ - see front matter © 2005 Elsevier B.V. All rights reserved.
doi:10.1016/j.geomorph.2005.07.028

Hicks et al. (1990) used sediment yields in the Southern Alps of New Zealand to challenge the long-held view that glaciers are the more effective erosion agents. Hallet et al. (1996) used a global data set to argue that glaciers are capable of eroding at significantly faster rates than rivers. Koppes and Hallet (2002) caution that the rates of glacial erosion inferred from total sediment budgets in recently deglaciated fjords are representative only of tidewater glaciers during post-Little Ice Age retreat. They estimate a recent mean rate of erosion of ~37 mm/year for the Muir Glacier, but suggest a long-term rate of ~7 mm/year, comparable to what can be achieved by rivers in some settings (Hallet et al., 1996).

Brozovic et al. (1997) were able to infer the relative efficacy of glacial erosion from topography. They examined various glaciated landscapes in the Nanga Parbat region of Pakistan that are being exhumed/uplifted at different rates. These different areas have similar landscapes with respect to the snowline, so the authors deduced that glaciers can maintain their elevation in the face of some of the most rapid rates of rock uplift on Earth, i.e., the glaciers can erode at least as rapidly as the uplift. Montgomery et al. (2001) suggested the same in their regional study of the Andes.

Braun et al. (1999) and Tomkin and Braun (2002) have developed the first 2-D model of landscape evolution that incorporates fluvial and glacial erosion. They have used this model to demonstrate the cycle of relief changes associated with glacial–interglacial cycles and, thus, how the patterns and rates of fluvial and glacial erosion differ. This model relies, however, on several parameters that have not been measured directly in the field. The model is built around the shallow ice approximation for the ice dynamics (e.g., Paterson, 1994). This is a simplification whereby the longitudinal stresses are neglected; i.e., it is assumed that the surface and bed slopes are parallel (e.g., Wettlaufer, 2001). This is only really applicable to large ice caps. Therefore, some aspects of erosion patterns in alpine glacial settings cannot be captured by the Braun et al. (1999) model.

As an alternative to estimating the rates of glacial erosion using sediment yields, interpretation of landforms, or glacial landscape evolution models, we suggest that it is informative to exploit our understanding of the characteristic form of fluvial landscapes. In this study we compare observed glaciated landscapes with estimations of how the (fluvial) landscape might look now had glaciers never developed. Extension of this approach to how the landscape would have looked prior to the onset of glaciation would require improved understanding of the response of fluvial erosion to climate change and a field site with a well-constrained history of base-level. Nevertheless, the approach described here allows us to evaluate how mountain ranges have evolved because of the onset of alpine glaciation. Prior work applying this approach in the eastern Sierra Nevada indicated that the primary impact of glaciers in small catchments has been above the mean Quaternary equilibrium line altitude (ELA), lowering valley floors and ridgelines (Brocklehurst and Whipple, 2002). (As described by Porter (1989), the mean Quaternary ELA represents 'average' Quaternary climatic conditions, midway between the current and last glacial maximum (LGM) ELAs. Glaciated landscapes often reflect erosion principally under these 'mean' conditions.) This paper presents a comprehensive evaluation of the technique. We compare our results from the smaller basins on the eastern side of the Sierra Nevada with basins of a similar size and at a similar latitude on the western side of the Sangre de Cristo Range of southern Colorado (Fig. 1). We also extend our analyses to some larger drainage basins, on both sides of the Sierra Nevada (Fig. 1).

2. Methods

2.1. DEM analyses

A flow routing routine in Arc/Info was used to extract drainage networks from USGS 30 m digital elevation models (DEMs), and these in turn were used to generate longitudinal profiles (along the line of greatest accumulation area) for each drainage basin. This approach has been demonstrated to be at least as accurate as obtaining longitudinal profiles from topographic maps (Snyder et al., 2000; Wobus et al., in press). The downstream extent of each drainage basin was taken to coincide with the range front, to exclude the alluvial/debris flow fan regime, and allow consistent comparison between basins. The extent of glaciation at the last glacial maximum (LGM), from field mapping and aerial photograph interpretation of terminal moraines, was used as a proxy to categorise the degree of glacial modification in each drainage basin (Brocklehurst and Whipple, 2002). Basins were separated into three categories, nonglaciated basins with essentially no glacial modification and no evidence of LGM moraines, partially glaciated basins, where LGM moraines lie some distance above the drainage basin outlet (subdivided into minor, moderate and significant), and fully glaciated basins, where the

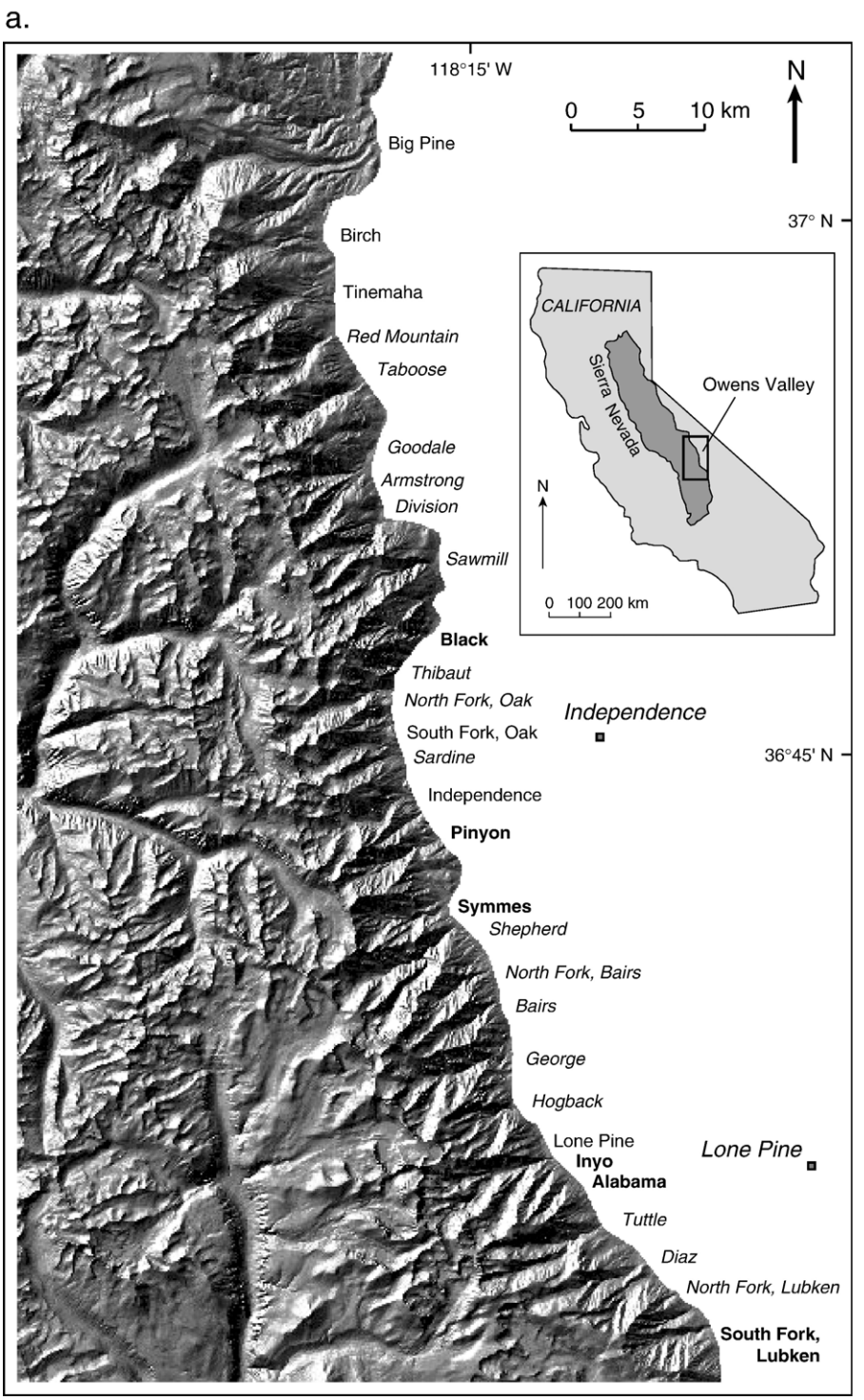

Fig. 1. (a) Shaded relief map (illuminated from the northwest) of the study site in the eastern Sierra Nevada, California, highlighted on the inset map. On the eastern side of the range, three categories of basin, based on the degree of glaciation at the Last Glacial Maximum (see Section 2.1), are illustrated as follows: nonglaciated (bold), partial glaciation (italic) and full glaciation (regular). Big Pine Creek is a 'large' fully glaciated basin, whereas the remainder of the fully glaciated basins are 'small' (see text). (b). Shaded relief map (illuminated from the northwest) of the study site on the western side of the Sangre de Cristo Range, Colorado, highlighted on the inset map. Three categories of basin, based on the degree of glaciation at the Last Glacial Maximum, are illustrated as follows: nonglaciated (bold), partial glaciation (italic) and full glaciation (regular). (c). Shaded relief map (illuminated from the northwest) of the Kings River basin, on the western side of the Sierra Nevada, highlighting tributaries discussed in the text.

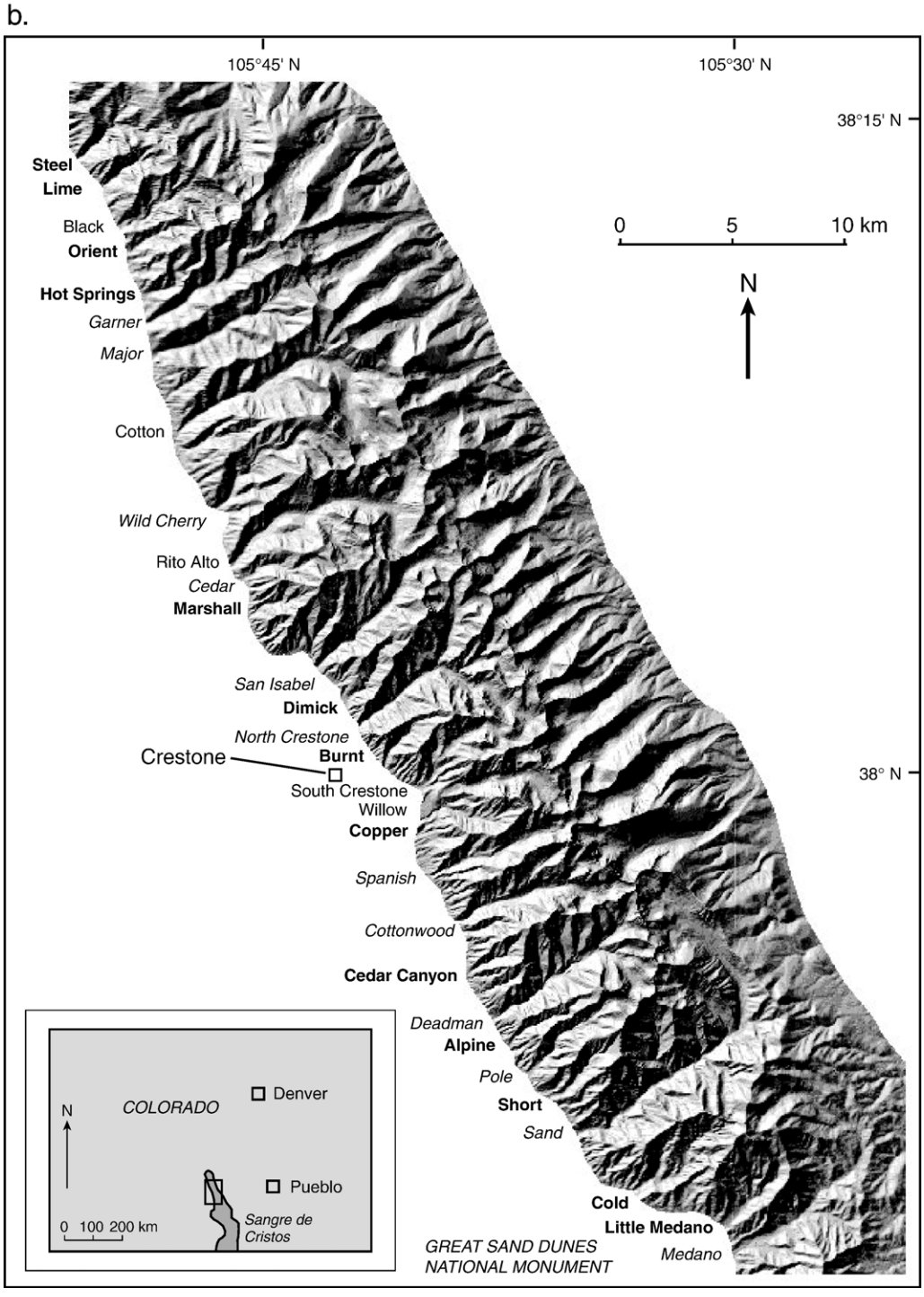

Fig. 1 (*continued*).

LGM moraines are at the drainage basin outlet. Subsequent analyses and modelling were carried out using Matlab scripts.

Fig. 2 compares representative longitudinal profiles of smaller drainage basins from the Sangre de Cristo Range (Fig. 2b) with those in the Sierra Nevada

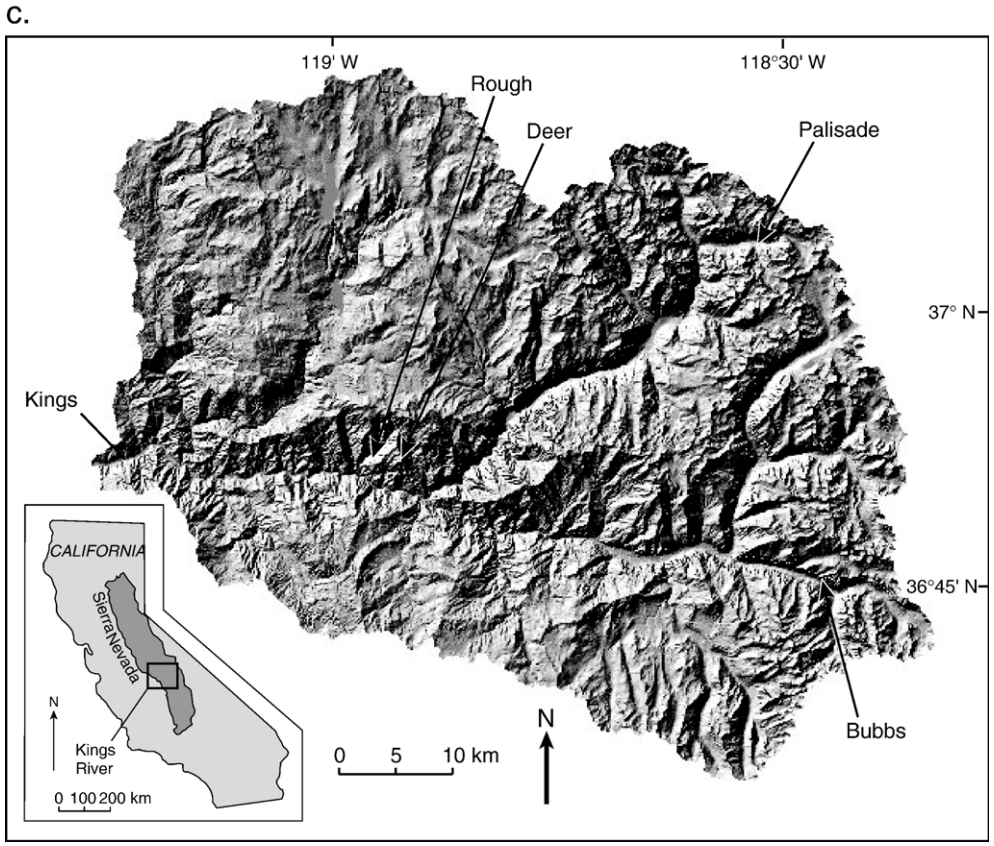

Fig. 1 (*continued*).

(Fig. 2a) (Brocklehurst and Whipple, 2002). In both ranges, the longitudinal profiles of nonglaciated basins look much like those seen in entirely unglaciated ranges (e.g., the Appalachians of Virginia and Maryland (Hack, 1957; Leopold et al., 1964), the King Range, northern California (Snyder et al.,

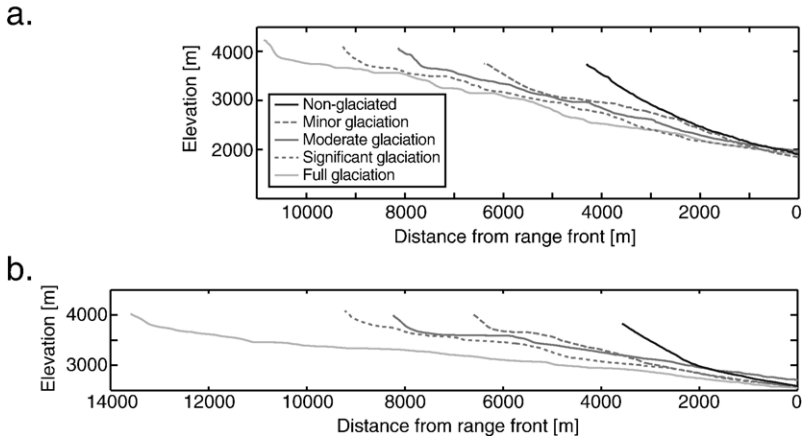

Fig. 2. Comparison of longitudinal profiles in the Sangre de Cristo Range and the eastern Sierra Nevada. (a) Sierra Nevada: longitudinal profiles from Alabama Creek (nonglaciated, black), Division Creek (minor glaciation, medium grey, dashed), Red Mountain Creek (moderate glaciation, medium grey, solid), Tuttle Creek (significant glaciation, medium grey, dotted) and Lone Pine Creek (full glaciation, light grey). No vertical exaggeration. (b) Sangre de Cristo: longitudinal profiles from Lime Creek (nonglaciated, black), Pole Creek (minor glaciation, medium grey, dashed), Wild Cherry Creek (moderate glaciation, medium grey, solid), Cottonwood Creek (significant glaciation, medium grey, dotted) and Rito Alto Creek (full glaciation, light grey). No vertical exaggeration.

2000), and the San Gabriel Mountains, southern California (Wobus et al., in press)). Increasing glacial influence is manifested as the development of a flatter section in the upper reaches of the profile, while the lower parts retain the shape of an unglaciated stream. Full glaciation produces upper reaches with long, shallow sections separated by steeper steps, although the lower regions still resemble the profiles of fluvial streams. Fig. 2a and b are at the same scale, and with no vertical exaggeration. The key difference between the longitudinal profiles of the Sangre de Cristo Range and the eastern Sierra Nevada is the reduced elevation range between the divide and the range front in the Sangre de Cristo Range, which in turn means that the average gradient of the Sangre de Cristo Range profiles is shallower.

2.2. Model calibration

The application of a fluvial landscape model here, to represent how the landscape might look now had glaciers never developed, exploits the fact that most fluvial landscapes around the world have a very similar morphology (smooth, concave longitudinal profiles), which can be described using the power-law relationship between local slope, S, and drainage area, A (Fig. 3, Flint, 1974):

$$S = k_s A^{-\theta}. \quad (1)$$

This relationship is observed in fluvial systems in numerous locations around the world, whether bedrock, mixed or alluvial channels, and (with the obvious exception of large knickpoints) whether at steady-state or not (e.g., Flint, 1974; Montgomery and Foufoula-Georgiou, 1993; Snyder et al., 2000; Tarboton et al., 1991; Willgoose, 1994). Under the special conditions of steady state (erosion rate equal to uplift rate at all points) the concavity, θ, and steepness, k_s, can be related to the parameters of erosion models for bedrock channels (e.g., Whipple and Tucker, 1999). In this case, however, because we are essentially just extrapolating modern topography, to reproduce topography similar to the current state of the nonglaciated basins, we do not need to concern ourselves with whether or not the modern topography (or our simulated topography) represents steady state in this sense. Similarly, this model also has no direct link to timescales or initial conditions; we only need to assume that the now-glaciated basins would have had sufficient time to respond in the same way as the currently nonglaciated basins. Indeed, because this effort

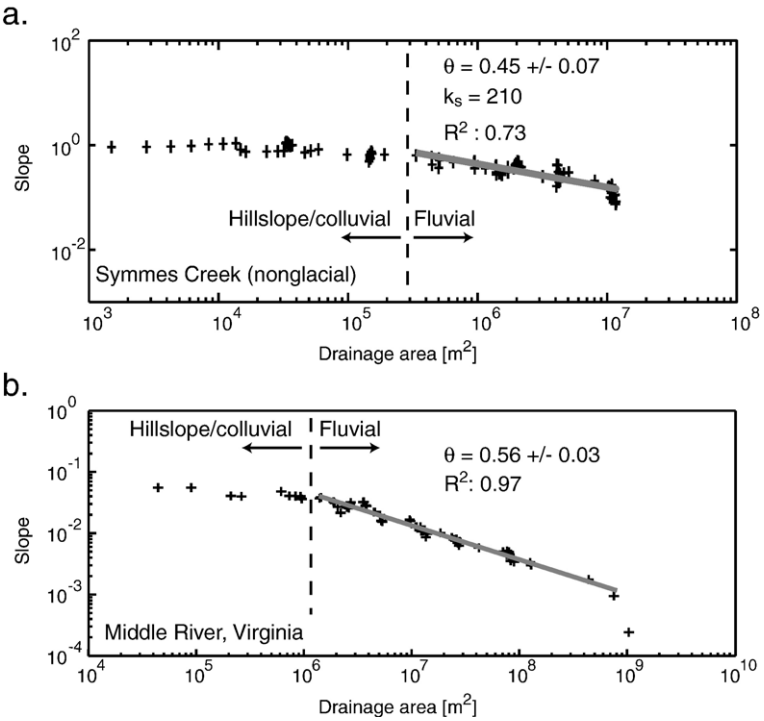

Fig. 3. Slope–area plots, indicating reaches dominated by hillslope/colluvial and fluvial processes (e.g., Snyder et al., 2000). (a) Symmes Creek, Sierra Nevada, a representative example from the nonglaciated basins in the study area used to constrain the fluvial simulation model. (b) Middle River, Virginia, illustrating the slope–area relationship over a significantly broader range of drainage area than the extrapolation employed here.

is a purely morphological approach, it is not even a concern if the dominant erosional process in some of the drainage basins is scour by debris flows rather than fluvial erosion (e.g., Stock and Dietrich, 2003). We simulate realistic modern fluvial topography for the glaciated basins by integrating (1) with mean values of θ and k_s determined from nonglaciated drainage basins within the same area. The only assumption necessary is that the slope–area relationship for the nonglaciated basins (e.g., Fig. 3a, drainage area $\sim 10^7$ m^2) can be extrapolated to the greater drainage area of the glaciated basins ($<5\times10^8$ m^2). Previous studies have demonstrated such a power-law relationship over larger ranges of drainage area (e.g., Baldwin et al., 2003; Tarboton et al., 1991; Whipple and Tucker, 1999; Wobus et al., in press), as shown in Fig. 3b. We used only data from trunk streams in our calculations for the 1-D simulations, and data from the whole drainage basin for our 2-D simulations. We calculated the steepness and concavity by linear regression in log–log space for each of the nonglacial basins, following techniques described by Snyder et al. (2000) and Wobus et al. (in press). We excluded hillslopes and debris-flow dominated colluvial channels from the regression, and calculated slopes on interpolated 10 m contour intervals. By selecting the downstream extent of the nonglaciated basins at the range front, we avoided regions of significant alluviation. Because θ and k_s are related, to determine a representative k_s we employed a mean value for θ from all of the nonglacial basins and repeated the regression for each basin to determine a normalised steepness index, k_{sn} (Snyder et al., 2000; Wobus et al., in press). The error-weighted mean values for θ and k_{sn} that were used in the simulations are given in Table 1.

Table 1
1-D calibration parameters for all nonglaciated drainage basins within the study areas, with $\pm$ 1σ errors

Basin	θ	ln k_{sm}
Eastern Sierra Nevada		
Alabama	0.32 ± 0.07	3.38 ± 1.60
Black	0.20 ± 0.07	3.49 ± 1.67
Inyo	0.37 ± 0.06	3.41 ± 1.59
Pinyon	0.19 ± 0.06	3.41 ± 1.72
South Fork, Lubken	0.45 ± 0.08	3.34 ± 1.57
Symmes	0.37 ± 0.05	3.32 ± 1.68
Mean	0.32 ± 0.11	3.39 ± 1.60
Sangre de Cristo		
Alpine	0.20 ± 0.08	2.95 ± 1.39
Burnt	0.37 ± 0.06	3.00 ± 1.38
Cedar Canyon	0.44 ± 0.06	3.05 ± 1.39
Cold	0.36 ± 0.05	3.01 ± 1.44
Copper	0.33 ± 0.06	3.16 ± 1.41
Dimick	0.21 ± 0.06	2.94 ± 1.40
Hot Spring	0.26 ± 0.07	2.99 ± 1.38
Lime	0.19 ± 0.13	3.02 ± 1.42
Little Medano	0.27 ± 0.05	2.94 ± 1.43
Marshall	0.45 ± 0.06	3.16 ± 1.36
Orient	0.31 ± 0.08	2.79 ± 1.38
Short	0.38 ± 0.06	3.14 ± 1.40
Steel	0.24 ± 0.08	2.92 ± 1.45
Mean	0.32 ± 0.10	3.01 ± 0.97
Western Sierra Nevada		
Boulder	0.46 ± 0.18	4.40 ± 1.66
Deer	0.37 ± 0.05	5.00 ± 1.72
Kennedy	0.28 ± 0.03	4.71 ± 1.62
Middle	0.33 ± 0.02	5.10 ± 1.67
Monarch	0.44 ± 0.02	4.48 ± 1.61
Rough1[a]	0.44 ± 0.02	5.11 ± 1.67
Rough2[a]	0.52 ± 0.02	4.99 ± 1.75
Rough3[a]	0.48 ± 0.03	4.99 ± 1.75
Rough4[a]	0.65 ± 0.04	5.02 ± 1.72
Mean	0.42 ± 0.11	4.92 ± 1.60

k_{sm} calculated using the calculated mean value of θ for each study area.
[a] Tributaries to Rough Creek.

2.2.1. 1-D simulations

Simply using extracted drainage area data to reconstruct a fluvial profile from (1) would produce sharp breaks at every tributary junction. Therefore, to rewrite (1) to obtain an analytical solution, we carried out a similar regression to determine a Hack law constant, k_h, and exponent, h (Hack, 1957), in the following relationship between drainage area and downstream distance, x, for each of the glacially modified basins:

$$A = k_h x^h. \quad (2)$$

Then for each of the glacially modified basins we integrated the slope–area relationship:

$$S = -\mathrm{d}z/\mathrm{d}x = k_s k_h^{-\theta} x^{-h\theta}. \quad (3)$$

This implicitly assumes that basin shape has not been significantly modified by glacial erosion. Although cirque development may result in widening in the headwaters (Oskin and Burbank, 2002) or elongation of the basin by headwall erosion (Brocklehurst and Whipple, 2002), we do not see evidence of substantial change in basin shape in our field sites, either from interpretation of topographic maps or in our calculated parameters for the Hack law. We set a maximum permitted hillslope and colluvial channel slope at the channel head of 40°, determined from slope histograms for nonglaciated basins. In practice this choice has little impact on the overall results, because the hillslope/colluvial reach represents a very short section of the profile as a whole. We fixed the simulated outlet ele-

vation to match the observed outlet elevation, reasoning that the glacial system has had very little opportunity to modify this elevation by either erosion (very short ice residence time in this region even for the fully glaciated cases) or by deposition (most of the sediment continues to the alluvial/debris flow fans below (Whipple and Trayler, 1996), and beyond). This is consistent with (i) the observation (Fig. 2) that, especially in the smaller basins, the lower portions of glaciated basin longitudinal profiles have smooth concave forms rather than stepped profiles, and (ii) the close match between the lower parts of the observed and simulated profiles in the smaller basins (see below).

A complication in larger glaciated basins concerns the amount of sediment in the lower reaches of these basins, i.e., the current streams contain more alluvium. In these cases it is not appropriate to employ the slope–area relationship calibrated in bedrock-channel dominated basins, because the alluviated channel will tend to have a shallower slope. In practice the simulated profile lies above the observed profile at every location in the basin except at the outlet, where the two are forced to match. This issue is addressed by shortening the simulated profile from the downstream end, such that the observed and simulated profiles are tied at the base of the bedrock channel reach rather than at the outlet. This results in a reach over which the observed and simulated profiles match well, before diverging farther upstream. On the eastern side of the Sierra Nevada and in the Sangre de Cristo Range we have field evidence for the location of the bedrock–alluvial transition, while on the western side of the Sierra Nevada this introduces some uncertainty into the analysis.

2.2.2. 2-D simulation

To extend the comparison between simulated fluvial and observed glacial landscapes beyond the longitudinal profile, we employed a 2-D model of landscape evolution. Then, following the sub-ridgeline relief method (Brocklehurst and Whipple, 2002), we mathematically stretched a smooth surface across the drainage basin from the ridgelines on one side to the other. From this ridgeline-related surface, we could extract directly a projection of the ridgelines onto the longitudinal profile, for the observed and simulated landscapes, to evaluate how the ridges and peaks have responded to the onset of glaciation. We selected the Geologic-Orogenic Landscape Evolution Model (GOLEM, Tucker and Slingerland, 1994, 1997) to simulate most-likely present-day fluvial landforms. GOLEM incorporates tectonic uplift, weathering, hillslope transport, landsliding, bedrock channel erosion, and sediment transport. This list comprises the most important landscape-forming processes in environments where chemical weathering is not significant. Bedrock channel erosion in GOLEM follows a shear-stress-derived power-law relationship (e.g., Howard et al., 1994; Whipple and Tucker, 1999). We fix the basin outline and initial drainage pattern to match the current topography, to allow direct comparison between simulated and observed topography. The alternative, allowing the drainage pattern to develop of its own accord from random perturbations in the initial topography, hinders subsequent comparison with observed landscapes. By fixing the basin outline we do not allow for the possibility that glaciers have been responsible for changing the shape of the basin. We run the landscape evolution model to a steady-state condition to reproduce a slope–area relationship of the form shown in (1); we are not necessarily suggesting or requiring that the nonglaciated basins in this part of the Sierra Nevada or the Sangre de Cristo Range are in steady state. In so doing, because we are not concerned directly with timescales, our choices for uplift rate, U, the fluvial erosion parameter, K, and the drainage area and slope exponents, m and n respectively, are not crucial, as long as the concavity and steepness values are appropriate. (At steady state, $k_s=(U/K)^{1/n}$ and $\theta=m/n$ (e.g., Whipple and Tucker, 1999)). Instead of using mean values for nonglaciated concavity and steepness calculated from the longitudinal profile data only, we calculated values using basinwide data, i.e., local slope and drainage area data from every point in each of the nonglaciated drainage basins. Comparisons of longitudinal profiles taken from our 2-D simulations with our 1-D results, however, show very minor differences.

3. Field sites

The field sites were selected because they exhibit a range of degrees of glacial modification amongst neighbouring drainage basins, from nonglaciated basins, essential to the modelling approach, to basins where LGM glaciers extended to the outlet. The field sites also have uniform climate and tectonic histories, and, as far as possible, uniform lithology. Accordingly, we selected the eastern side of the Sierra Nevada, adjacent to the Owens Valley (Fig. 1a), the western side of the Sangre de Cristo Range in southern Colorado (Fig. 1b), and the Kings River basin on the western side of the Sierra Nevada (Fig. 1c). Overall, our data set comprises 68 smaller drainage basins ($<4\times10^7$ m^2), including those used to calibrate the fluvial model (Table 1), and 4 larger drainage basins ($>10^8$ m^2). Ideally more larger basins would allow a more substantial compari-

son, but this represents the extent of basins sufficiently close to our other basins to allow the application of the calibrated model of the fluvial landscape (our results are consistent across all 4 basins, lending confidence that we have captured the major differences between small and large catchments).

On the eastern side of the Sierra Nevada, we examined two large basins, Big Pine Creek and Bishop Creek, in addition to the 28 smaller basins previously described (Brocklehurst and Whipple, 2002). The current form of the Sierra Nevada was produced by normal faulting and westward tilting, beginning at ~5 Ma (Wakabayashi and Sawyer, 2001). The range front fault system that forms the eastern scarp may still be active, contributing to modest rates of uplift (0.2–0.4 mm/year, Gillespie, 1982; Le, 2004). The tectonic regime of the western side of the Sierra Nevada is generally thought to be a tilting crustal block (e.g., Huber, 1981); Tertiary stream gradients were lower than modern ones (Wakabayashi and Sawyer, 2001). This section of the Sierra Nevada comprises regionally homogeneous Cretaceous granodiorites and quartz monzonites (Bateman, 1965; Moore, 1963, 1981; Stone et al., 2001). On the eastern side of the range, the side-by-side occurrence of catchments ranging from those displaying essentially no glacial modification to those with major glacial landforms allows quantitative description of fluvial landscapes in this environment, and estimation of how the neighbouring glaciated basins would look now had glaciers never developed. Drainage networks on the western slope are substantially larger. We focussed on the Palisade and Bubbs tributaries in the Kings River drainage, which lies opposite the portion of the eastern side of the range studied. Because of the extensive glacial modification of the upper portion of the basin, we calibrated the erosion model using smaller tributaries to the Kings River farther downstream (Fig. 1c), and streams in the adjacent Kaweah River basin.

The western side of the Sangre de Cristo Range (Fig. 1b) comprises Paleozoic sedimentary units and Precambrian metamorphic rocks, which strike parallel to the range (Johnson et al., 1987). The tectonic regime is consistent throughout the region of interest. The normal component of slip rates on the range front fault system has averaged around 0.1–0.2 mm/year during the late Pleistocene (McCalpin, 1981, 1986, 1987), comparable to, if somewhat lower than, rates measured in the eastern Sierra Nevada. As in the eastern Sierra Nevada, the occurrence of neighbouring glacial and nonglacial basins allows local calibration of the model of fluvial erosion. Our study in the Sangre de Cristo Range examined 31 small ($<4\times10^7$ m^2) drainage basins.

4. Results

4.1. Smaller basins

The simulation work on the fluvial landscape, presented by Brocklehurst and Whipple (2002), illustrated how some of the smaller, glaciated basins of the eastern Sierra Nevada might look now had glaciers never developed. Here, we compare these results with those obtained from the western Sangre de Cristo Range.

The first step in using the approach described here is to verify that we can reproduce realistic nonglacial topography for an individual basin using fluvial simula-

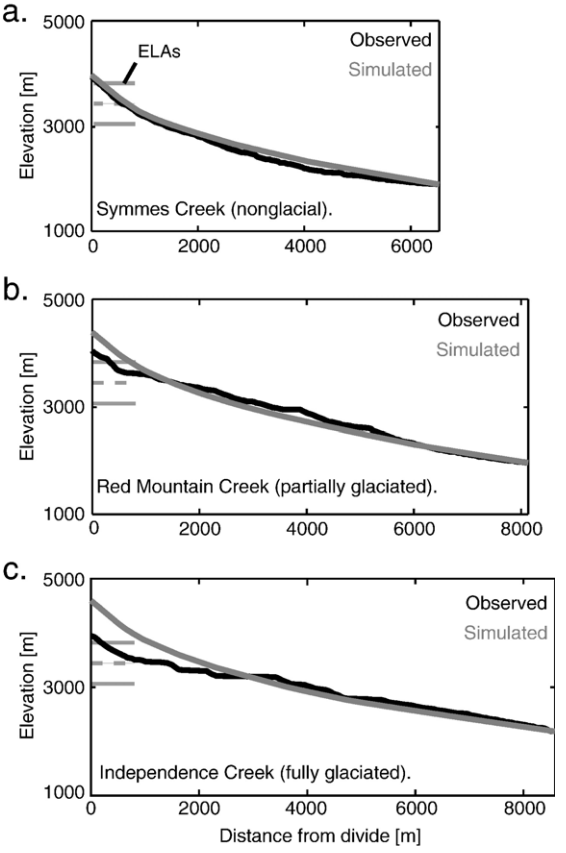

Fig. 4. Representative one-dimensional simulated profiles for small basins in the Sierra Nevada study area. (a) Symmes Creek, a nonglaciated basin. The darker line is the longitudinal profile extracted from the DEM, and the paler line is the simulated longitudinal profile. Horizontal lines are the modern (top), mean Quaternary (dashed) and LGM (bottom) ELAs at the range crest (Burbank, 1991). Notice the close agreement between the simulated and observed profiles for this representative example. (b) Red Mountain Creek, a partially glaciated basin. Key as for Symmes Creek. (c) Independence Creek, a small, fully glaciated basin. Key as for Symmes Creek. Notice the very close agreement between the observed and simulated profiles below the mean Quaternary ELA, and especially below the LGM ELA.

tion, which uses mean values of θ and k_{sn} from a series of nonglaciated basins (Table 1). As shown in Figs. 4a and 5a, this is achieved in the Sierra Nevada and the Sangre de Cristo Range. Focussing on the cases where we do not see evidence of significant headwall erosion, the principal difference between how the glaciated basins might have looked and the current appearance is at higher elevations (Figs. 4b, c and 5b, c). Here, glaciers have carved large cirque basins and lowered and flattened the valley floors. Furthermore, the 2-D simulations allow us to infer the response of the ridgelines, and indicate that in both ranges the glaciers have brought down the ridgelines by an amount commensurate with the valley floor incision (Fig. 6). Thus, no significant (more than 100 m) relief generation occurred in terms of missing mass (Brocklehurst and Whipple, 2002).

At lower elevations, below the mean Quaternary ELA, the difference between the simulated and observed longitudinal profiles and ridge lines is minor, indicating little glacial incision of the valley floor (Figs. 4 and 5), despite the clear U-shaped cross section to the valleys (Figs. 7 and 8). This suggests that glaciers carried out minimal downward cutting below the mean ELA during the LGM (when some of the glaciers extended to the range front), even though they were active in widening the valley. The major difference between the results from the eastern Sierra Nevada and the western Sangre de Cristo Range is that there is less drainage basin relief in the Sangre de Cristo Range, so overall gradients are shallower. This is also shown in the nonglacial calibration data (Table 1); the mean concavities in the two ranges are essentially identical, but mean normalised steepness is less in the Sangre de Cristo Range. Otherwise, the results from the two ranges are quite comparable, despite the major contrast in lithology, and lesser differences in climate and tectonic setting.

As discussed by Brocklehurst and Whipple (2002), in some cases the simulated profile lies at a lower elevation than the observed profile. The simplest interpretation of this is that the river would have incised

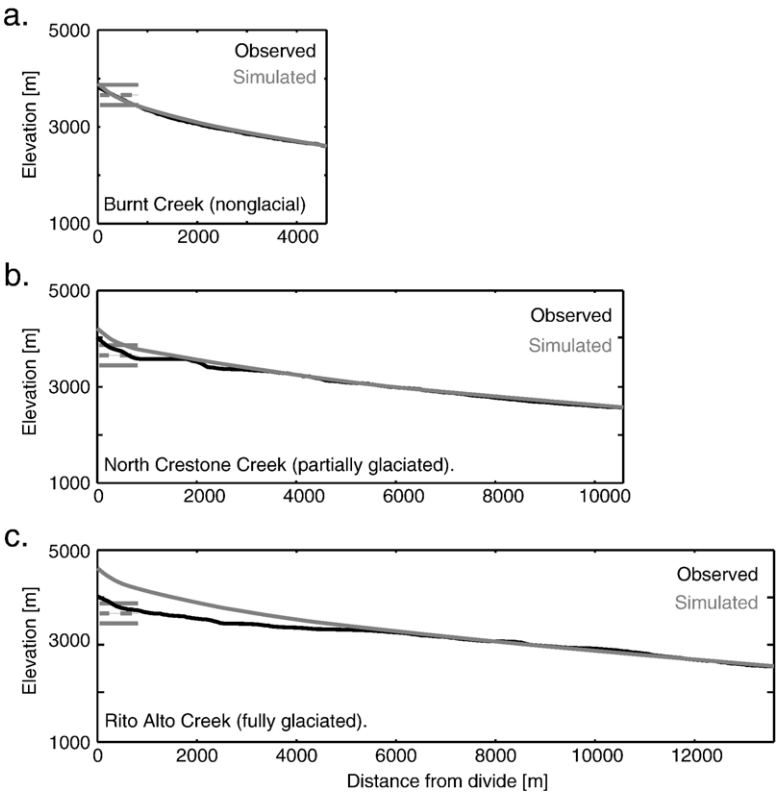

Fig. 5. Representative one-dimensional simulated profiles from the Sangre de Cristo. (a) Burnt Creek, a nonglaciated basin. The darker line is the longitudinal profile extracted from the DEM, and the paler line is the simulated longitudinal profile. Horizontal lines are the modern (top), mean Quaternary (dashed) and LGM (bottom) ELAs at the range crest (McCalpin, 1981). Notice the close agreement between the simulated and observed profiles for this representative example. (b) North Crestone Creek, a partially glaciated basin. Key as for Burnt Creek. (c) Rito Alto Creek, a small, fully glaciated basin. Key as for Burnt Creek. As in the Sierra Nevada (Fig. 3), notice the very close agreement between the observed and simulated profiles below the mean Quaternary ELA, and especially below the LGM ELA.

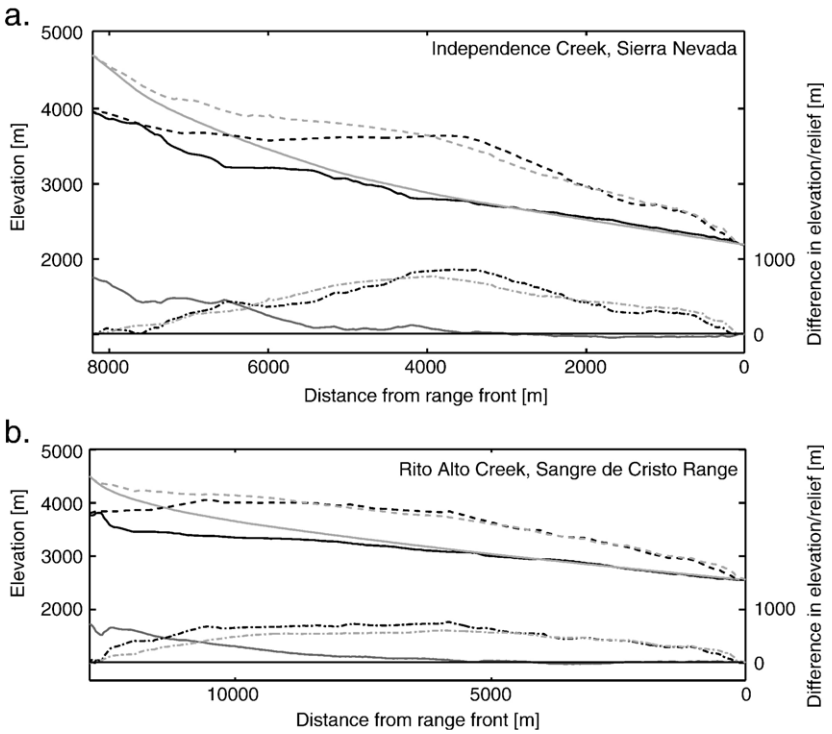

Fig. 6. Two-dimensional simulations of (a) Independence Creek, Sierra Nevada, and (b) Rito Alto Creek, Sangre de Cristo Range. Longitudinal profiles drawn from the present topography (black) and simulated topography (pale grey) with the difference between the two in dark grey. Also shown are the interpolated ridgeline surfaces along the profiles (present topography—black, dashed; simulated topography—pale grey, dashed), with the relief calculated as the difference in elevation between the interpolated ridgeline and the valley floor (dot-dash lines). ELAs indicated as in Figs. 3 and 4. Comparing the observed and simulated topography, the valley floor and the ridgeline agree well at lower elevations and then diverge considerably higher up, with the simulated ridgeline and longitudinal profile considerably higher. We suggest that the valley floor and the ridgelines have been lowered by glacial erosion.

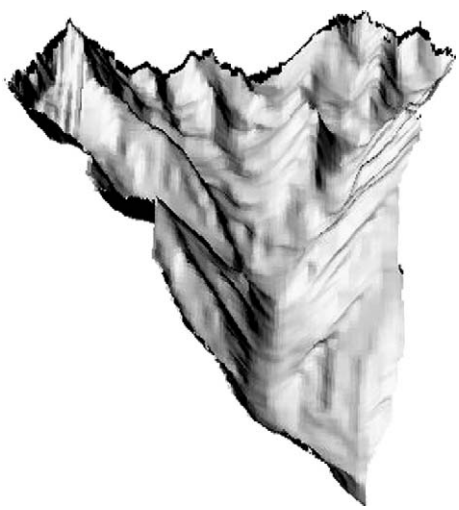

Fig. 7. 3-D view of shaded relief image draped on topography of Independence Creek, showing the same extent as the longitudinal profile (Fig. 3c). The valley floor is wide and flat, and the valley cross section is U-shaped almost to the basin outlet.

Fig. 8. 3-D view of shaded relief image draped on topography of Rito Alto Creek, Sangre de Cristo Range.

farther had glaciers not developed upstream. Given that we have observed several streams in the Sierra Nevada still flowing over glacially polished bedrock, we doubt that fluvial erosion outpaces glacial here. Alternatively, some local complication, such as harder lithology, might cause deviation from the expected profile. In the case of the Sierra Nevada, though, the granite is essentially uniform in strength, and no systematic lithologic changes are associated with regions where the simulated profile lies at a lower elevation than the

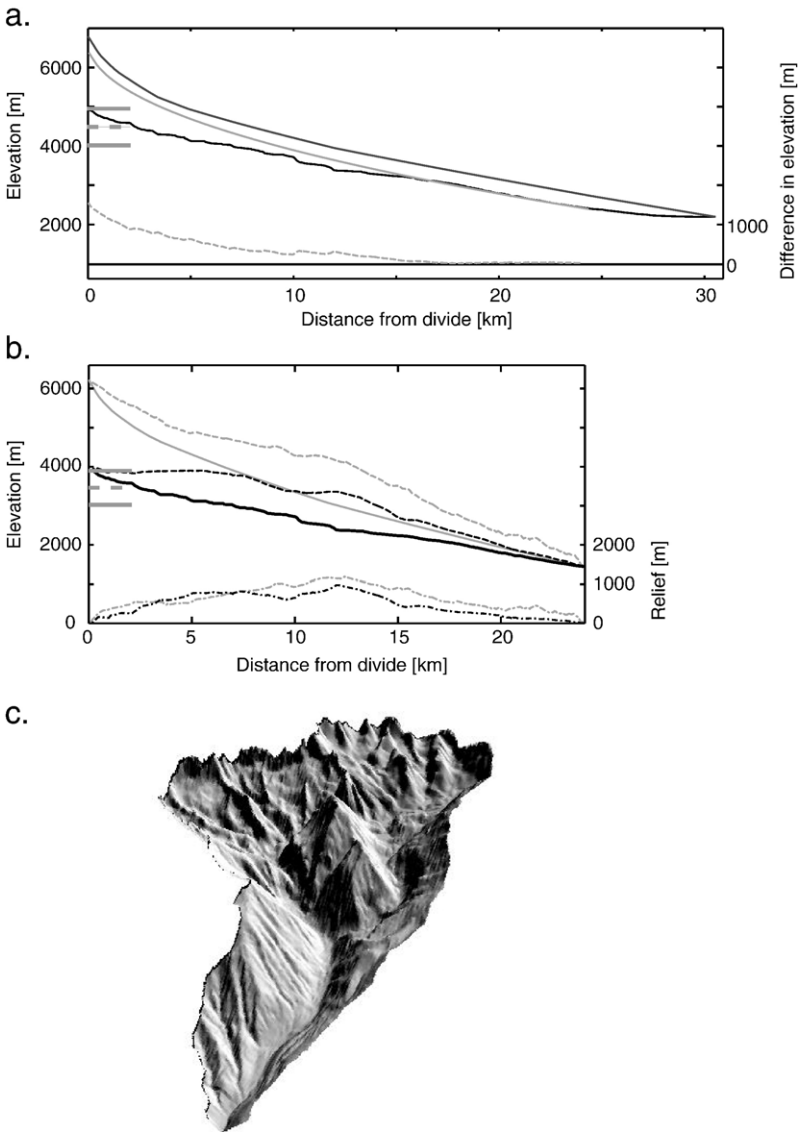

Fig. 9. (a) One-dimensional simulated profiles for Big Pine Creek, a large, fully glaciated basin. The black line is the longitudinal profile extracted from the DEM, the dark grey line is a simulated longitudinal profile for the full length of the basin, the pale grey line is a simulated profile shortened from the foot of the valley to account for alluviation, and the dashed line is the difference between the observed and simulated profiles. Horizontal lines are the modern (top), mean Quaternary (dashed) and LGM (bottom) ELAs at the range crest (Burbank, 1991). (b) Longitudinal profiles extracted from 2-D GOLEM simulation for the non-alluviated portion of Big Pine Creek. Present topography (black) and simulated topography (pale grey) with interpolated ridgeline surfaces along the profiles, dashed, and the relief, measured as the difference in elevation between interpolated ridgeline and valley floor, as a dot-dash line. ELAs as in (a). Comparing the observed and simulated topography, the valley floor and the ridgeline agree well at lower elevations and then diverge considerably higher up, with the simulated ridgeline and longitudinal profile considerably higher. Distribution of relief, however, is similar in the two cases. We suggest that the valley floor and the ridgelines have been lowered by glacial erosion. (c) 3-D perspective view of shaded relief draped on topography for Big Pine Creek. Glacial steps in the valley floor (indicated) continue close to the mouth of the valley, along with extensive glacial modification in the upper parts of the basin.

observed one. Consequently, our preferred interpretation is that the glaciers have been responsible for headwall retreat/headwater widening (consistent with patterns of divide migration). This means that our simulated fluvial profile is too long (and thus has too great a drainage area) to represent how a never-glaciated profile would look now, so has an overall slope that is too shallow. Brocklehurst and Whipple (2002) estimated the magnitude of headwall erosion, in addition to that which would have occurred under continuous fluvial conditions, by shortening the simulated profile until a good match was achieved over the reach where the observed profile has a concave, step-free shape. In addition to examples from the Sierra Nevada (Brocklehurst and Whipple, 2002), headwall erosion is also evident in the Sangre de Cristo Range (Brocklehurst, 2002).

4.2. Large basins

Fig. 9 illustrates what happens when we extend our analyses to larger basins, using Big Pine Creek in the Sierra Nevada as an example, and again using the mean concavity and normalised steepness values for the eastern Sierra Nevada given in Table 1. Attempting to fit the entire length of the basin produces a 1-D simulated profile (Fig. 9a) that lies significantly above the observed profile at every point upstream of the outlet. The simplest interpretation of this is that the glacier here has incised more rapidly than a river would have done at every point along the longitudinal profile. We suggest, however, that this is not quite accurate; the lower reaches of Big Pine Creek are quite alluviated, and so trying to simulate an alternative profile with a slope–area relationship calibrated on bedrock channels is inappropriate. When we look at only that portion of the profile with some amount of bedrock in the channel, as indicated by field observations, we obtain a reasonable fit to a short section of the profile. Significant differences from the smaller glaciated basins studied previously, however, are apparent. Deviation between the simulated profile and the observed profile occurs far below the mean Quaternary ELA, even below the LGM ELA. Here, and also in Bishop Creek, the large glaciers have incised the valley floor at much lower elevations than in the smaller basins, even though the glaciers did not extend much farther beyond the range front (Fig. 1). As in the smaller glaciated basins, the 2-D simulation (Fig. 9b) shows that the ridgelines have closely followed the response of the longitudinal profile, and, thus, no major relief production occurred. Fig. 9c illustrates, in 3-D, the glacial modification of the longitudinal profile far below the ELA. Although the smaller basins in the Sierra Nevada show U-shaped cross sections in the lower part of the basin (Fig. 7), only in the larger basins is this accompanied by the incision of dramatic glacial steps.

Fig. 10 illustrates 1-D simulations from the Bubbs and Palisade Creek tributaries to the Kings River using mean concavity and normalised steepness values from the basins listed in Table 1. These simulations highlight deviations from a smooth, concave longitudinal profile at several points. Towards the outlet, these may reflect an alluvial channel. Glacial steps are clearly pronounced far below the LGM ELA and suggest deep glacial scour all the way to the LGM terminus. Considering that our DEM-derived profiles reflect surface elevation rather than the elevation of bedrock beneath the potentially deep fills of glacial scours, this is consistent with the well-known observations of overdeepenings near glacial termini in Yosemite Valley and the Hetch Hetchy in the Sierra Nevada (e.g., Gutenberg et al., 1956; MacGregor et al., 2000), and glaciated basins in the Wind River Range, Wyoming, and Glacier National Park, Montana. A component of headwall erosion, particularly in Bubbs Creek, might also need to be addressed (Brocklehurst and Whipple, 2002). The scale of the basins on the western side of the Sierra Nevada, however, means that we are pushing the limits of what we can learn using this simulation technique. Calibrating the model on the western side of the range is hindered by greater glacial modification of the landscape, making nonglaciated basins more elusive. Stepped profiles on the western side of the range may also reflect lithologic variations, which are much more pronounced than on the eastern side of the range (e.g., Wahrhaftig, 1965).

5. Discussion and conclusions

5.1. Summary of results

We have found very similar results applying our fluvial landscape simulation technique to the eastern Sierra Nevada and the western Sangre de Cristo Range. In small drainage basins, glaciers have incised substantially in cirque floors, but ridgelines have also been lowered, so relief production is minor. Glacial incision below the mean ELA is also modest, despite obvious valley widening. The principal difference between the two ranges is that more total relief occurs in the Sierra Nevada, so observed and simulated profiles are steeper. In detail, the two landscapes exhibit subtle differences, such as lithology exerting an influence on valley cross-sectional form in the Sangre de Cristo Range

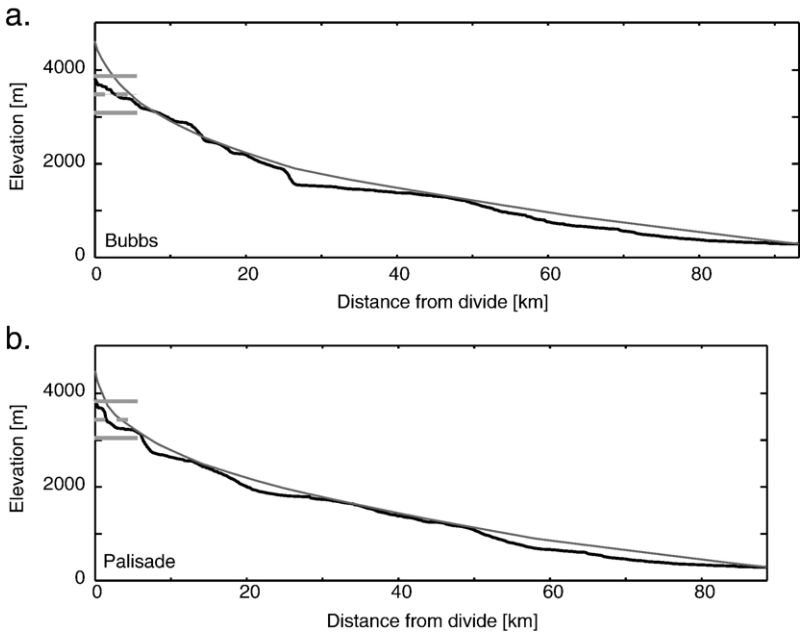

Fig. 10. (a) One-dimensional simulated profiles for Bubbs Creek, glaciated tributary to the Kings River. Observed profile is in black, simulated profile in grey. Horizontal lines are the modern (top), mean Quaternary (dashed) and LGM (bottom) ELAs at the range crest (Burbank, 1991). (b) One-dimensional simulated profiles for Palisade Creek, glaciated tributary to the Kings River. Key as for Bubbs Creek; headwall erosion is 2 km in this case. All simulated profiles have much higher divides than the observed profile, and glaciated steps in the observed profile are observed far below the ELA.

(Brocklehurst, 2002). The consistent results demonstrate, however, that this approach provides valuable insight into the role of glaciers in sculpting mountain ranges.

5.2. Implications for glacial erosion processes

Comparing, for example, Figs. 6 and 9b, these simulation studies have clearly demonstrated that the pattern of erosion by large glaciers is quite different from that by smaller glaciers. Large glaciers can erode more rapidly, particularly in the ablation zone, than smaller glaciers. Such a situation was also discussed by Hallet et al. (1996), who noticed that yields from glacial erosion tend to increase with basin size. This they presumed to reflect an increase in effective rates of erosion from small cirque glaciers to large, fast-moving valley glaciers. We see major variations amongst valley glaciers within a small range of drainage basin sizes, which suggest that something more subtle is happening. The following constitutes speculation on what differences in glacial processes might be responsible. The principal distinctions of the larger basins are that they have a larger accumulation area and that they would have had a lower overall slope prior to the onset of glaciation. In the smaller, steeper basins, the glaciers may be little more than thin bodies of ice advancing rapidly downvalley, with subglacial water percolating out readily. This is crucial, because fluctuations in subglacial water pressure are thought to play a key role in erosion by quarrying (Alley et al., 1999; Hallet, 1996; Hooke, 1991). Our field observations suggest that quarrying is the major glacial erosion process in the eastern Sierra Nevada. Striations are present, but the major features of bedrock outcrops on the valley floor are the stepped granite sheets, where blocks approximately 50 cm thick have been removed. If subglacial water is readily flushed out, pressure fluctuations will not develop, and erosion by quarrying, and, therefore, mean rates of erosion, may be restricted. Shallower slopes may also allow more complicated subglacial water systems, associated with enhanced fluctuations in pore water pressure, again favouring quarrying and more rapid erosion (Hallet, 1996). Moreover, the larger accumulation area will result in substantially greater ice discharge. Because most formulations for glacial erosion, whether through abrasion or quarrying, emphasise the importance of ice velocity, this may allow more rapid erosion. The larger accumulation area also allows the glacier to extend farther down the valley for more extended periods of time, permitting greater glacial erosion. The causes of the obvious distinctions between

small basins, normally occupied by modest cirque glaciers, and large drainages featuring larger valley glaciers represent an important focus for future research.

A final question of the dynamics of glacial erosion is why the smaller glaciers widen the valley floor without incising. As demonstrated by Harbor (1992), starting from an initial V-shaped cross section, erosion driven by ice velocity will be focussed initially towards the development of a U-shaped cross section. It is possible that, because of the short residence times of these glaciers at the full LGM extents (Porter, 1989), the glaciers have not yet been able to pass out of this stage. We suggest that subglacial water may again play a crucial role. The subglacial water along the steep thalweg is likely to form a well-connected network for much of the annual cycle and reduce the possibility of large fluctuations in water pressure (Hallet, 1996; Hooke, 1991). Along the glacier margins, the subglacial drainage network may not be as well developed, while crevasses will allow meltwater to percolate to the base, potentially allowing greater water pressure fluctuations, and, thus, more rapid erosion. Meanwhile, as described above, larger glaciers may be more capable of incision along the thalweg along with valley widening. We, thus, highlight the role of subglacial water in erosion processes as a key focus for future research.

This study suggests that a range of possible responses exists for glacial erosion systems of different scales. Initial efforts on constructing evolution models for the glacial landscape have focussed on the larger scale end of the spectrum (Braun et al., 1999; MacGregor et al., 2000; Merrand and Hallet, 2000; Oerlemans, 1984). Predictions of these models include large overdeepenings below the long-term ELA, in addition to overdeepenings associated with tributary junctions. Further development of these models, to capture the full diversity of glacial landscapes, will lead to a more complete understanding of glacial erosion.

5.3. Limitations and future applications of the technique

The principal limitation on comparing fluvial landscapes with observed glacial landscapes to deduce the effects of glacial erosion on a mountain belt is the requirement that the fluvial landscapes must be in close proximity to the glacial ones. This stems from a current inability to precisely predict parameters in fluvial erosion formulations based purely on a set of climatic, tectonic and lithologic observations. Only at higher latitudes have glaciers sculpted every basin within a mountain range. The work presented here has demonstrated the applicability of our approach in two ranges with different lithologies and somewhat different climates and tectonic settings.

This analysis exploits the fact that we understand the characteristics of fluvial landscapes better than glaciated landscapes. As yet we are unable to use this approach to establish convincingly how the range might have looked prior to glaciation, because of (i) uncertainty over how θ and k_s respond to climate change (e.g., Roe et al., 2002; Whipple et al., 1999); and (ii) lack of detailed understanding of the base-level history over the Quaternary (for instance, how the Owens Valley fell with respect to the Sierra Nevada (Gillespie, 1982), and how the San Luis Valley fell with respect to the Sangre de Cristo Range (e.g., McCalpin, 1981)). Understanding the response of rivers to climate change during the Quaternary would allow us to predict how mountain ranges would have looked prior to the onset of glaciation, while the ability to constrain model parameters of erosion purely on the basis of climatic, tectonic and lithologic parameters would allow application of this approach where local calibration of the fluvial erosion model is not possible.

The application of a single calibration leads to problems when the valley floor encompasses alluvial and bedrock reaches. This can be solved in larger basins, where alluviation is a natural consequence of steadily increasing drainage area, by restricting the analysis to the bedrock portions of the profile. Where a small stream is choked by debris from the last glaciation, as in the eastern Sangre de Cristo Range, however, a realistic model fit is not possible because of the close proximity of the morainal debris, occasional bedrock reaches, and the glacially modified upper section. Accordingly, the analysis was restricted to the western side of the Sangre de Cristo Range.

If fluvial and glacial basins with similar tectonics and precipitation can be found, this approach would allow us to compare the responses of rivers and glaciers to rapid tectonic uplift, for example in the Southern Alps of New Zealand. Preliminary results using this approach in the Manaslu region of the Himalayas (Whipple and Brocklehurst, 2000) emphasised the ability of glaciers to maintain a shallow gradient in spite of rapid uplift, unlike their fluvial counterparts (Brocklehurst, 2002; Brozovic et al., 1997).

Acknowledgements

This work was supported by NSF Grant EAR-9980465 (to KXW), a NASA Graduate Fellowship, a GSA Fahnestock Award, and a CIRES Visiting Fellow-

ship (all to SHB). Thorough, constructive reviews by Eric Leonard and an anonymous reviewer helped greatly to clarify the manuscript.

References

Alley, R.B., Strasser, J.C., Lawson, D.E., Evenson, E.B., Larson, G.J., 1999. Glaciological and geological implications of basal-ice accretion in overdeepenings. In: Mickelson, D.M., Attig, J.W. (Eds.), Glacial Processes Past and Present, Geological Society of America Special Paper. Geological Society of America, Boulder, Colorado, pp. 1–9.

Baldwin, J.A., Whipple, K.X., Tucker, G.E., 2003. Implications of the shear-stress river incision model for the timescale of post-orogenic decay of topography. Journal of Geophysical Research 108 (B3). doi:10.1029/2001JB000550.

Bateman, P.C., 1965. Geology and tungsten mineralization of the bishop district, California. U.S. Geological Survey Professional Paper 470 (208 pp.).

Braun, J., Zwartz, D., Tomkin, J.H., 1999. A new surface-processes model combining glacial and fluvial erosion. Annals of Glaciology 28, 282–290.

Brocklehurst, S.H., (2002). Evolution of Topography in Glaciated Mountain Ranges. PhD Thesis, Massachusetts Institute of Technology, Cambridge, MA. 236 pp.

Brocklehurst, S.H., Whipple, K.X., 2002. Glacial erosion and relief production in the eastern Sierra Nevada, California. Geomorphology 42 (1–2), 1–24.

Brozovic, N., Burbank, D.W., Meigs, A.J., 1997. Climatic limits on landscape development in the northwestern Himalaya. Science 276, 571–574.

Burbank, D.W., 1991. Late quaternary snowline reconstructions for the southern and central Sierra Nevada, California and a reassessment of the "recess peak glaciation". Quaternary Research 36, 294–306.

Flint, J.J., 1974. Stream gradient as a function of order, magnitude, and discharge. Water Resources Research 10, 969–973.

Gillespie, A.R., 1982. Quaternary Glaciation and Tectonism in the Southeastern Sierra Nevada, Inyo County, California. PhD Thesis, California Institute of Technology, Pasadena. 695 pp.

Gutenberg, B., Buwalda, J.P., Sharp, R.P., 1956. Seismic explorations on the floor of Yosemite Valley, California. Geological Society of America Bulletin 67, 1051–1078.

Hack, J.T., 1957. Studies of longitudinal stream profiles in Virginia and Maryland. U.S. Geological Survey Professional Paper 294-B, 97.

Hallet, B., 1996. Glacial quarrying: a simple theoretical model. Annals of Glaciology 22, 1–8.

Hallet, B., Hunter, L., Bogen, J., 1996. Rates of erosion and sediment evacuation by glaciers: a review of field data and their implications. Global and Planetary Change 12, 213–235.

Harbor, J.M., 1992. Numerical modeling of the development of U-shaped valleys by glacial erosion. Geological Society of America Bulletin 104, 1364–1375.

Hicks, D.M., McSaveney, M.J., Chinn, T.J.H., 1990. Sedimentation in proglacial Ivory lake, Southern Alps, New Zealand. Arctic and Alpine Research 22, 26–42.

Hooke, R.L., 1991. Positive feedbacks associated with erosion of glacial cirques and overdeepenings. Geological Society of America Bulletin 103, 1104–1108.

Howard, A.D., Dietrich, W.E., Seidl, M.A., 1994. Modeling fluvial erosion on regional to continental scales. Journal of Geophysical Research 99, 13971–13986.

Huber, N.K., 1981. Amount and timing of late Cenozoic uplift and tilt of the central Sierra Nevada, California—evidence from the upper San Joaquin river. U.S. Geological Survey Professional Paper 1197 (28 pp.).

Johnson, B.R, Lindsey, D.A. Bruce, R.M., Soulliere, S.J., 1987. Reconnaissance geologic map of the Sangre de Cristo Wilderness Study Area, south-central Colorado. USGS Miscellaneous Field Studies Map, MF-1635-B.

Koppes, M.N., Hallet, B., 2002. Influence of rapid glacial retreat on the rate of erosion by tidewater glaciers. Geology 30 (1), 47–50.

Le, K., 2004. Late Pleistocene to Holocene extension along the Sierra Nevada range front fault zone, California. MSc thesis Thesis, Central Washington University.

Leopold, L.B., Wolman, M.G., Miller, J.P., 1964. Fluvial Processes in Geomorphology. W.H. Freeman, San Francisco. 522 pp.

McCalpin, J.P., 1981. Quaternary geology and neotectonics of the west flank of the northern Sangre de Cristo Mountains, south-central Colorado. Doctoral Thesis, Colorado School of Mines, Golden, CO. 287 pp.

McCalpin, J.P., 1986. Quaternary tectonics of the Sangre de Cristo and villa grove fault zones. Special Publication - Colorado Geological Survey 28, 59–64.

McCalpin, J.P., 1987. Recurrent quaternary normal faulting at major creek, Colorado: an example of youthful tectonism on the eastern boundary of the Rio Grande rift zone. In: Beus, S.S. (Ed.), Geological Society of America Centennial Field Guide—Rocky Mountain Section. Geological Society of America, pp. 353–356.

MacGregor, K.C., Anderson, R.S., Anderson, S.P., Waddington, E.D., 2000. Numerical simulations of glacial valley longitudinal profile evolution. Geology 28 (11), 1031–1034.

Merrand, Y., Hallet, B., 2000. A physically based numerical model of orogen-scale glacial erosion: importance of subglacial hydrology and basal stress regime. GSA Abstracts with Programs 32 (7), A329.

Molnar, P., England, P., 1990. Late Cenozoic uplift of mountain ranges and global climate change: chicken or egg? Nature 346, 29–34.

Montgomery, D.R., Foufoula-Georgiou, E., 1993. Channel network source representation using digital elevation models. Water Resources Research 29 (12), 3925–3934.

Montgomery, D.R., Balco, G., Willett, S.D., 2001. Climate, tectonics and the morphology of the Andes. Geology 29 (7), 579–582.

Moore, J.G., 1963. Geology of the mount Pinchot quadrangle, southern Sierra Nevada, California. US Geological Survey Bulletin 1130 (152 pp.).

Moore, J.G., 1981. Geologic map of the Mount Whitney quadrangle, Inyo and Tulare Counties, California, GQ-1545. US Geological Survey Map.

Oerlemans, J., 1984. Numerical experiments on large-scale glacial erosion. Zeitschrift fuer Gletscherkunde und Glazialgeologie 20, 107–126.

Oskin, M., Burbank, D.W., 2002. Geomorphic evolution of steady-state in a glaciated mountain range: kyrgyz range, Western Tien Shan. Eos, Transactions of the American Geophysical Union 83 (47), F1325.

Paterson, W.S.B., 1994. The Physics of Glaciers. Pergamon, Oxford, OX, England. ix, 480 pp.

Porter, S.C., 1989. Some geological implications of average quaternary glacial conditions. Quaternary Research 32, 245–261.

Raymo, M.E., Ruddiman, W.F., 1992. Tectonic forcing of late Cenozoic climate. Nature 359, 117–122.

Raymo, M.E., Ruddiman, W.F., Froelich, P.N., 1988. Influence of late Cenozoic mountain building on ocean geochemical cycles. Geology 16, 649–653.

Roe, G.H., Montgomery, D.R., Hallet, B., 2002. Effects of orographic precipitation variations on the concavity of steady-state river profiles. Geology 30 (2), 143–146.

Snyder, N.P., Whipple, K.X., Tucker, G.E., Merritts, D.J., 2000. Landscape response to tectonic forcing: DEM analysis of stream profiles in the Mendocino triple junction region, northern California. Geological Society of America Bulletin 112 (8), 1250–1263.

Stock, J., Dietrich, W.E., 2003. Valley incision by debris flows: evidence of a topographic signature. Water Resources Research 39 (4). doi:10.1029/2001WR001057.

Stone, P., Dunne, G.C., Moore, J.G., Smith, G.I., 2001. Geologic Map of the Lone Pine 15' Quadrangle, Inyo County, California. U.S. Geological Survey Geologic Investigations Series, I-2617: Online version 1.0.

Tarboton, D.G., Bras, R.L., Rodriguez-Iturbe, I., 1991. On the extraction of channel networks from digital elevation data. Hydrological Processes 5, 81–100.

Tomkin, J.H., Braun, J., 2002. The influence of alpine glaciation on the relief of tectonically active mountain belts. American Journal of Science 302, 169–190.

Tucker, G.E., Slingerland, R.L., 1994. Erosional dynamics, flexural isostasy, and long-lived escarpments: a numerical modeling study. Journal of Geophysical Research 99 (B6), 12229–12243.

Tucker, G.E., Slingerland, R.L., 1997. Drainage basin responses to climate change. Water Resources Research 33, 2031–2047.

Wahrhaftig, C., 1965. Stepped topography of the Southern Sierra Nevada, California. Geological Society of America Bulletin 76, 1165–1190.

Wakabayashi, J., Sawyer, T.L., 2001. Stream incision, tectonics, uplift, and evolution of topography of the Sierra Nevada, California. Journal of Geology 109, 539–562.

Wettlaufer, J.S., 2001. Dynamics of snow and ice masses. Lecture Notes in Physics 582, 211–217.

Whipple, K.X., Brocklehurst, S.H., 2000. Estimating glacial relief production in the Nepal Himalaya. GSA Abstracts with Programs 32, A320.

Whipple, K.X., Trayler, C.R., 1996. Tectonic control of fan size: the importance of spatially variable subsidence rates. Basin Research 8, 351–366.

Whipple, K.X., Tucker, G.E., 1999. Dynamics of the stream-power river incision model: implications for height limits of mountain ranges, landscape response timescales, and research needs. Journal of Geophysical Research 104, 17661–17674.

Whipple, K.X., Kirby, E., Brocklehurst, S.H., 1999. Geomorphic limits to climate-induced increases in topographic relief. Nature 401, 39–43.

Willgoose, G., 1994. A statistic for testing the elevation characteristics of landscape simulation models. Journal of Geophysical Research 99 (B7), 13987–13996.

Wobus, C. et al., in press. Tectonics from topography: Procedures, promise and pitfalls. In: S.D. Willett, N. Hovius, M. Brandon, D. Fisher (Eds.), GSA Penrose Special Paper: Tectonics, Climate and Landscape Evolution.